PNAS
www.pnas.org

Supplementary Information for

Drastic enhancement of crystal nucleation in a molecular liquid by its liquid-liquid transition

Rei Kurita and Hajime Tanaka

Hajime Tanaka.
E-mail: tanaka@iis.u-tokyo.ac.jp

This PDF file includes:

Supporting Information Text

1. Key experimental protocol for separating the thermodynamic factors of crystal nucleation from its kinetic factor

Here we describe a special experimental protocol, which was used to study effects of order-parameter fluctuations associated with LLT on crystal nucleation in TPP. First we equilibrated a liquid at 303 K above $T_{\rm m}$, and rapidly cooled it to an annealing temperature $T_{\rm a}$ with a rate of 100 K/min. If we anneal TPP at $T_{\rm a}$ near but above the spinodal temperature $T_{\rm SD} = 215.5$ K, fluctuations of S is enhanced until a system reaches a quasi-equilibrium state. Then we heated the sample to $T_{\rm x}$ with a heating rate of 100 K/min and observed nucleation of crystals. When crystal nucleation happens within ∼100 s at $T_{\rm x}$ (e.g., at 235 K), S fluctuations still remain and thus assist crystal nucleation. Then, we count the number of nuclei as a function of time and estimate the crystal nucleation frequency.

The very existence of such a quasi-equilibrium state is a consequence of separation between the time required for reaching the local quasi-equilibrium state and that required for nucleation of liquid II to take place. By checking behaviors for a few different waiting times, we found that annealing a sample for 5 min at $T_{\rm a}$ is enough to attain a quasi-equilibrium state of liquid I at $T_{\rm a}$ (see Fig. 2). Above but near $T_{\rm SD}$, nucleation of liquid II occurs after an incubation time. However, we confirmed that the incubation time is much longer than 5 min. Thus, we conclude that our sample has order-parameter (S) fluctuations but is free from nuclei of liquid II. This is our method for preparing a sample with quasi-equilibrium S fluctuations at each annealing temperature $T_{\rm a}$. Then, we heat the sample with S fluctuations from $T_{\rm a}$ to the crystallization temperature $T_{\rm x}$ with a rate of 100 K/min by using the hotstage. The longest time required for heating from $T_{\rm a}$ to $T_{\rm x}$ was less than 20 s. This time is much shorter than the decay time of S fluctuations and thus the S fluctuations induced by annealing at $T_{\rm a}$ should remain after heating.

However, S fluctuations formed at $T_{\rm a}$ should decay eventually since $T_{\rm x}$ is far from $T_{\rm SD}$. Thus, the next key question is whether S fluctuations can survive until crystal nucleation is initiated at $T_{\rm x}$. We confirmed that nucleation of crystals at $T_{\rm x} = 235$ K occurs very quickly and after a few minutes we can clearly see crystal nuclei with optical microscopy. On noting the growth velocity of a crystal is about 0.1 μm/s at 235 K, the birth of crystal nuclei should occur about a minute after the temperature jump (see Fig. 1). We also confirmed that the growth speed of crystals does not depend on the annealing temperature $T_{\rm a}$, since crystallization always takes place at the same temperature $T_{\rm x}$. Thus, we conclude that the incubation time of crystal nucleation is much shorter than the decay time of S fluctuations at $T_{\rm x}$. This conclusion is supported by a direct link between S fluctuations induced below $T_{\rm SD}$ and crystal nucleation at $T_{\rm x}$ shown in Fig. 5 as well as the systematic changes observed in our experiments (see the main text).

Furthermore, our method allows us to separate the thermodynamic factor (particularly, the liquid-crystal interfacial tension γ) of crystal nucleation from its kinetic factor (see equation (1)). We can control the amplitude of S fluctuations by changing $T_{\rm a}$. We note that the change in τ_t and $\delta\mu$ are too small to explain many orders of magnitude change in the crystal nucleation frequency. Enhancement of S fluctuations may influence τ_t and $\delta\mu$, but the effects should be minor. For example, since τ_t contributes to the nucleation frequency as a prefactor, its small change can never lead to many orders of magnitude change in the crystal nucleation frequency. We also note that our measurements of dielectric spectroscopy show that the influence of S fluctuations on the structural relaxation time is very minor even if it exists (1). Furthermore, the enthalpy change of liquid detected by DSC measurements is also negligibly small, indicating that the influence of S fluctuations on $\delta\mu$ should also be minor. Thus, we may assume that $\delta\mu$ depends only on $T_{\rm x}$. This is consistent with the fact that the growth velocity $\mathcal{V}$ is independent of $T_{\rm a}$ (note that $\mathcal{V}$ depends only on $\delta\mu$ (see equation (3))). Thus, we may conclude that any dependence of the crystal nucleation rate on $T_{\rm a}$ should originate largely from the influence of S fluctuations formed at $T_{\rm a}$ on γ.

2. Estimation of the crystal nucleation rate

Here we explain how we estimate the crystal nucleation rate J. The number of nuclei formed is strongly dependent on the annealing temperature $T_{\rm a}$. Thus, we changed the magnification used for microscopy observation. Accordingly, the field of view used was 128 μm × 100 μm for $T_{\rm a} = 216 \sim 217$ K, 288 μm ×216 μm for $T_{\rm a} = 218 \sim 220$ K, and a full circular window of the temperature-control hot stage, whose diameter is 1 mm, for $T_{\rm a} = 221 \sim 235$ K. The time duration to estimate J was set to 0.1 s for $T_{\rm a} = 216$ K, 1.0 s for $T_{\rm a} = 217$ K, and 10 s for all the other temperatures. For $T_{\rm a} \leq 225$ K the number of nuclei is always more than 25. For $T_{\rm a} \geq 225$ K, however, the number of nuclei becomes less than 10 even when we used the full window of 1 mm diameter for a thickness of 10 μm (see below about the thickness of samples), leading to a larger error. To reduce the statistical errors, we took average over 10 independent experiments for each $T_{\rm a}$.

As explained above, we used the different size of the field of view and the different time duration, depending on the annealing temperature $T_{\rm a}$. Then, we plot the number of nuclei as a function of time $t_{\rm w}$ in each image and determine J from the slope of its linear part. In Fig. S1, we explain how we estimated the crystal nucleation rate. The J was determined from the slope of the linear fit to the data between 100 s and 170 s, before the saturation due to interference between crystals takes place.

Here we also discuss whether our results reflect homogeneous nucleation of crystals or heterogeneous one induced by impurities or glass walls confining a sample. First we address the effect of glass walls of a sample cell. To check this issue, we made experiments by using three different sample thicknesses, 5, 10, and 20 μm and found that the number of nuclei is proportional to the sample thickness, or the sample volume (not the area), as shown in Fig. S1. This indicates that the crystal nucleation is 'not' induced by the glass surfaces. Next we discuss the effect of impurities on crystal nucleation. Nuclei formed in the very early stage might be induced by impurities and thus we ignore this very initial part (before 100 s), as shown in Fig. S1. If the nucleation were predominantly induced by impurities, it should not depend on $T_{\rm a}$ or $t_{\rm w}$. However, this is not the

case, as shown in the main text and Fig. S1, indicating that the nucleation basically takes place homogeneous in bulk under the influence of fluctuations of the order parameter S and is not affected by impurities.

Finally we consider a possibility that there are pre-existing crystal nuclei formed during annealing at T_a. To check such a possibility, we consider effects of the size distribution of crystal nuclei on the estimation of the nucleation rate (see Fig. S2). If there is a size distribution of nuclei, it should affect the timing at which we first detect crystal nuclei. For simplicity, let us suppose that there is some size distribution of nuclei formed at T_a, as shown in Fig. S2. When the system is heated to T_x, the nuclei are firstly detected after t_0, which is the incubation time for crystallization. Then the number of detected nuclei during Δt should be $\mathcal{V}\Delta t$, where $\mathcal{V}$ is the growth velocity at T_x. In this case, the nucleation frequency should be proportional to $\mathcal{V}$. However, we know from our previous work (2) that the growth speed of crystal nuclei is faster at 240 K (0.2 μm/s) than at 235 K (0.1 μm/s) . This means that J_0 should be larger at T_x=240 K than at T_x=235 K. But this is opposite to what we observed (see Fig. 3D). This suggests that the time delay caused by the size distribution of nuclei is negligible in our measurement time scale: such slight changes in the emergence time may matter only before 100 s (see Fig. S1). Thus we conclude that there are few effects of pre-existing nuclei on our estimation of J even if they exist. We infer that there may be no such pre-existing crystal nuclei after annealing at T_a in our experiments.

3. Prediction of the Classical Nucleation Theory (CNT)

The CNT prediction for crystal nucleation frequency is given by equation (1) in the main text. Thus, it can be expressed as

$$J = \frac{k_n}{\tau_t} \exp\left(-\frac{A}{T(T_m - T)^2}\right). \quad [S1]$$

where A is a parameter.

To make a comparison between the CNT prediction with the experimental data, we used the experimental data of dielectric spectroscopy to estimate the characteristic time of transport, τ_t (3), and $T_m = 295$ K. Then we made the fitting of equation (S1) to our experimental data above $T_a > 220$ K by using k_n and A as the fitting parameters. We note that at this temperature range, which is far above $T_{SD} = 215.5$ K, the effects of S fluctuations should be negligibly weak and we expect that the CNT describes the experimental data well. We obtained the best fit with $k_n = 0.198$ and $A = 3.5 \times 10^7$ (see Fig. 3D). Near T_m, the thermodynamic driving force, or the chemical potential difference between the crystal and liquid, disappears, whereas near T_g the mobility necessary for transport of a molecule from the liquid to the crystal is lost (or, τ_t steeply increases toward T_g. This leads to the typical bell shaped curve shown in Fig. 3D, which is universal to many systems (4). However, below $T_a = 220$ K, our experimental data for the systems annealed at T_a near T_{SD} significantly exceeds the CNT prediction, as shown in Fig. S3 and also in Fig. 3D: the magnitude of the deviation monotonically increases while approaching T_{SD} and almost reaches four orders of magnitude near T_{SD}. This strongly indicates the enhancement of the crystal nucleation rate by S fluctuations, which becomes more significant while approaching T_{SD}.

The crucial feature is the positive curvature of the temperature dependence of the crystal nucleation frequency. This can never be explained by the ordinary classical nucleation frequency scenario. The only possible explanation may be crystallization of two polymorphs with different melting points. To check such a possibility, we fit the following function to J.

$$J = \frac{k_{n1}}{\tau_t} \exp\left(-\frac{A}{T(T_m - T)^2}\right) + \frac{k_{n2}}{\tau_t} \exp\left(-\frac{B}{T(T_{m2} - T)^2}\right), \quad [S2]$$

where k_{n1}, k_{n2}, A, B, and T_{m2} are the fitting parameters. We use the same data (3) as above for τ_t. Although there is a systematic deviation, we can somehow fit the data with classical nucleation theory assuming the two types of polymorphs (see Fig. S4), using the following fitting parameters: $k_{n1} = 0.198$, $k_{n2} = 1.0 \times 10^7$, $A = 3.5 \times 10^7$, $B = 1.1 \times 10^7$, and $T_{m2} = 254.7$ K. However, this scenario can be clearly denied by the single melting behavior of only one type of crystal.

4. Another supporting evidence for the reduction of the crystal nucleation barrier by S fluctuations

Here we show crucial information obtained from calorimetric measurements, which not only provides further evidence for the reduction of the crystal nucleation barrier by S fluctuations but also allows us to separate the nucleation of crystals from their growth. In the experiments, we measured the heat flux during the transformation with a differential scanning calorimeter (Mettler Toledo, DSC-822e). We quenched TPP to $T_a = 213$ K ($< T_{SD}$), annealed it for t_w, and then measured the heat flux during the heating process with a rate of 20 K/min. Figure S5A shows the heat flux as a function of T upon heating. We observe only one peak (peak L) for the sample of $t_w = 0$ s, which corresponds to crystallization of TPP. As shown in Fig. S5A, this peak shifts towards a lower temperature with an increase in t_w, suggesting that the barrier for crystal nucleation is lower for the system annealed for a longer t_w. Since SD-type LLT proceeds at this annealing temperature $T_a = 213$ K ($< T_{SD}$) (2), the amplitude of S fluctuations should increase with t_w. Thus, this result indicates that the crystal nucleation barrier decreases as the amplitude of S fluctuations increases with t_w. This is consistent with our microscopy observation (see Fig. 5). In addition, the above result also rules out the possibility of formation of pre-existing nuclei. If we suppose that pre-existing nuclei are formed in the annealing process, we expect that crystal growth should start at the same temperature for different annealing periods and thus the DSC peak position should be the same.

For t_w longer than 10800 s, another peak (peak H) of the hear flux appears at a higher temperature and its peak height increases while accompanying the decrease of the height of peak L. Figure S5B shows the t_w-dependence of the peak temperatures

of both peak L and H. The peak temperature of peak L monotonically decreases with increasing t_w, whereas that of peak H stays constant. The t_w-dependences of the enthalpy change ΔH associated with peak L (ΔH_L), peak H (ΔH_H), and LLT (ΔH_{LLT}, not shown in Fig. S5*A*) are shown in Fig. S5*C*. The ΔH_L (circles) is almost constant for $t_w \leq 10800$ s, It suggests that $\delta\mu$ can be regarded as constant for $t_w \leq 10800$ s, whereas it monotonically decreases with an increase in t_w for $t_w > 10800$ s. On the other hand, both ΔH_H (triangles) and ΔH_{LLT} (solid line) increase with t_w. The summation of all these three contributions is constant, indicating the conservation of the total enthalpy change. It is worth noting that the t_w-dependence of ΔH_H is very similar to that of ΔH_{LLT}.

To further elucidate the nature of peak L and H, we heat liquid II, which is formed by annealing at $T_a = 213$ K for $t_w = 28800$ s, to 243 K, which is located just between peak L and H. Then we measure the enthalpy change during annealing at 243 K. The result is shown in Fig. S5*D*. We analyse the temporal evolution of the enthalpy during the annealing by fitting the Avrami-Kolmogorov equation, $\Delta H(t) = \Delta H_0[1 - \exp(-Kt^n)]$ (5), where ΔH_0 is the total enthalpy change and K and n are the fitting parameters. We obtain $n = 3$ and $K = 1.7 \times 10^{-12}$ s^{-3} from the fitting. This value of the Avrami exponent n means that crystallization proceeds with heterogeneous nucleation and the growth is three dimensional. This apparent heterogeneous nucleation is a consequence of the fact that crystal nuclei are already formed at 243 K and this heat evolution comes exclusively from the growth of these pre-existing nuclei. Thus, we conclude that peak L and peak H correspond to the nucleation of crystals and their growth, respectively. With this assignment, we can further conclude that the t_w-dependence of the peak temperature of peak L is a consequence of the fact that the barrier for crystal nucleation is lower for a sample with the larger amplitude of S fluctuations formed by longer annealing (i.e., longer t_w) below T_{SD}.

Here we consider why crystal nucleation and growth can be observed separately. The separation occurs at the onset of ΔH_H, which almost coincides with the onset of ΔH_{LLT}. After the increase of ΔH_H, the thermodynamic driving force for crystallization, $\delta\mu$, should decrease with an increase in the fraction of locally favored structures, S, since the free energy of the liquid should be lowered by the formation of locally favored structures (6). According to equations (1) and (3) of CNT in the main text, the nucleation of crystals is controlled by $\delta\mu$, γ, and τ_t, whereas the growth of crystals is governed solely by $\delta\mu$ and independent of γ. We already show the firm evidence for the fact that γ decreases with an increase in S in the liquid (see Fig. 5). The enhancement of crystal nucleation indicates that the decrease in γ overwhelms that in $\delta\mu$ in equation (1) in the main text. However, the decrease of $\delta\mu$ should also lead to the decrease in the crystal growth velocity $\mathcal{V}$ (see equation (3) in the main text). When liquid II becomes unstable during heating beyond the stability limit of liquid II, it transforms back to liquid I, resulting in the increase in $\delta\mu$. This should increase the crystal growth speed abruptly, leading to the emergence of peak H. More importantly, this separation between the nucleation and growth should also be induced by the abrupt change in the kinetic factor τ_t. The viscosity of TPP, or τ_t, is a very steep increasing function of S (2), and thus the kinetic factor is also strongly influenced by S. Thus, nuclei formed in high S regions should be difficult to grow because of both slow dynamics and small $\delta\mu$. However, the transformation from liquid II to liquid I (7), which takes place around the onset temperature of peak H, removes both causes of slow growth, leading to the steep increase in $\mathcal{V}$.

5. Incubation time of crystal nucleation for other materials without LLT

We measure the incubation time (instead of measuring the crystal nucleation rate by counting the number of nuclei at a function of time) of triphenyl phosphine (TPPN) and polyethylene glycol (PEG) since the crystal growth rates of these materials are very high (see Fig. S6). We note that the incubation time of crystal nucleation is proportional to the inverse of the nucleation rate. The open circle corresponds to the incubation time when TPPN is annealed and crystallized at $T_a = 295$ K. On the other hand, the filled symbols correspond to the incubation time at a fixed temperature T_x =295 K after the liquid is annealed at T_a for 5 min. These results clearly indicate that the incubation time is not affected by the annealing treatment at all. We also confirmed that the rate of crystal nucleation of PEG is also unchanged by the annealing at lower temperatures. There, the open circles correspond to the incubation time when the sample is annealed at T_a, while the filled circle symbols correspond to the incubation time at a fixed temperature $T_x = 333$ K after the sample is annealed at T_a for 3 min. We also confirmed that these results do not depend on the length of the annealing time.

References

1. Murata K, Tanaka H (2019) Link between molecular mobility and order parameter during liquid–liquid transition of a molecular liquid. *Proc. Natl. Acad. Sci. USA* 116(15):7176–7185.
2. Tanaka H, Kurita R, Mataki H (2004) Liquid-liquid transition in the molecular liquid triphenyl phosphite. *Phys. Rev. Lett.* 92:025701.
3. Schiener B, Loidl A, Chamberlin RV, Böhmer R (1996) Dielectric study of supercooled triphenylphosphite and butyronitrile: Comparison with a mesoscopic model. *J. Mol. Liq.* 69:243–251.
4. Kelton K, Greer AL (2010) *Nucleation in condensed matter: applications in materials and biology.* (Elsevier) Vol. 15.
5. Onuki A (2002) *Phase Transition Dynamics.* (Cambridge Univ. Press, Cambridge).
6. Tanaka H (2012) Bond orientational order in liquids: Towards a unified description of water-like anomalies, liquid-liquid transition, glass transition, and crystallization. *Eur. Phys. J. E* 35:113–196.
7. Kobayashi M, Tanaka H (2016) The reversibility and first-order nature of liquid–liquid transition in a molecular liquid. *Nature Commun.* 7:13438.

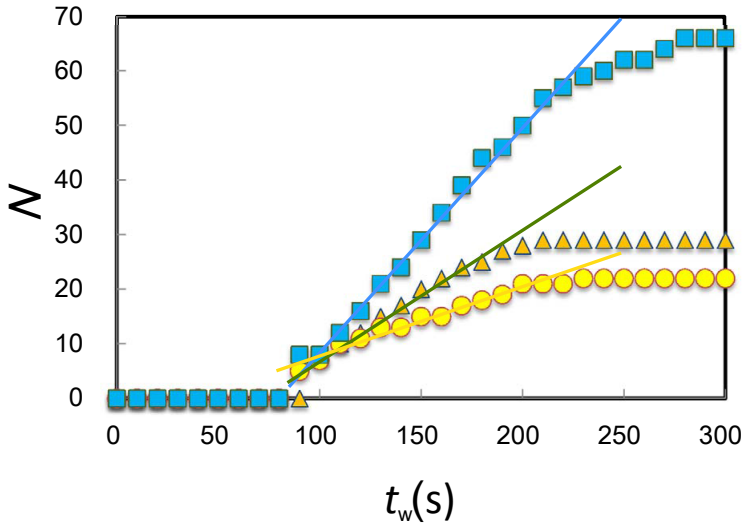

Fig. S1. An example of the estimation of the crystal nucleation rate at $T_x = 235$ K for a sample annealed at $T_a = 220$ K. The duration of the observation was until $t_w = 300$ s. The measurement area was 288 μm $\times$ 216 μm. Circles, triangles, and squares correspond to a sample of thickness d=5, 10, 20 μm, respectively. In this plot, the average was taken over 5 times for d =5 and 20 μ m, whereas 10 times for d =10 μm. The J was determined from the slope of the solid line fitted to the data between 100 s and 170 s before the saturation due to interference between crystals takes place. From the slope of the t-dependence of N, we obtain $J = 3.6 \times 10^{-7}$, 3.7×10^{-7}, and 3.6×10^{-7} (1/(μm^3·s)) for $d = 5$, 10, 20 μm. The absence of the sample thickness dependence indicates that crystal nucleation takes place homogeneously.

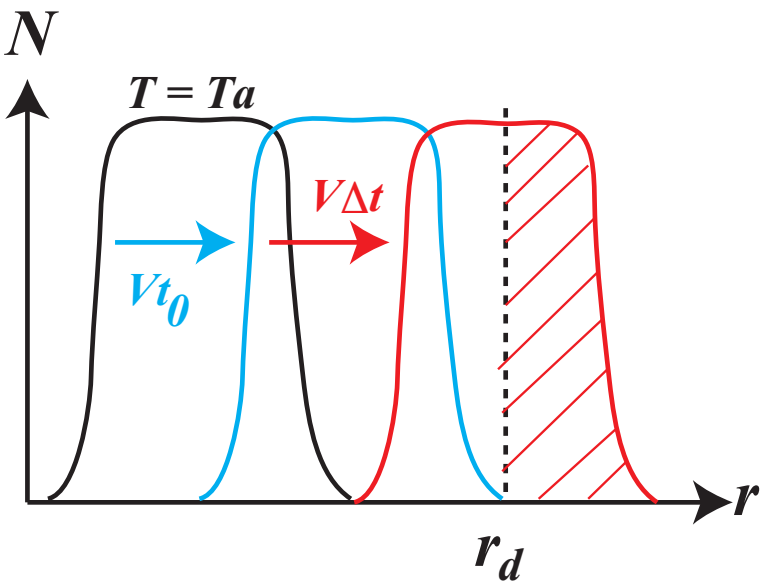

Fig. S2. Schematic graph for crystal nucleation and growth. r_d corresponds to a detectable radius. If the nuclei are created at $T_{\rm a}$, a histogram becomes the solid line. Then the crystal nuclei grow at $T_{\rm x}$ and the first nuclei can be detected at $t = t_0$, which corresponds to the incubation time. After that, the number of the detected crystal nuclei (summation of shaded domain) increases with proportional to $\mathcal{V}$. Thus the nucleation rate should be proportional to $\mathcal{V}$ if the nuclei is pre-existed at $T_{\rm a}$.

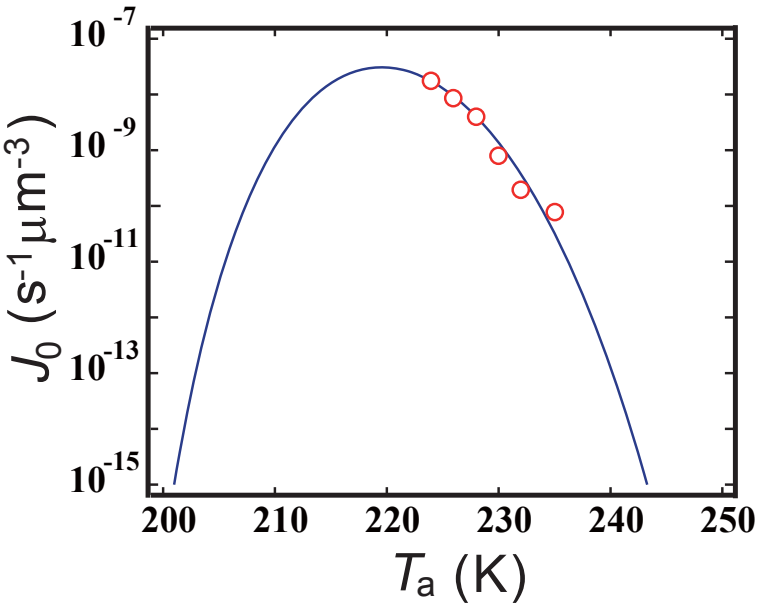

Fig. S3. The prediction of the classical nucleation theory (CNT) and its comparison with the experimental data. The CNT prediction (the solid curve) describes the experimental data very well above $T_{\rm a} > 220$ K. However, as shown in Fig. 3D, the nucleation rate of the annealed samples far exceeds the CNT prediction below this temperature. This strong deviation from the CNT prediction (nearly four orders of magnitude near $T_{\rm SD}$) should come from the enhancement of crystal nucleation by S fluctuations.

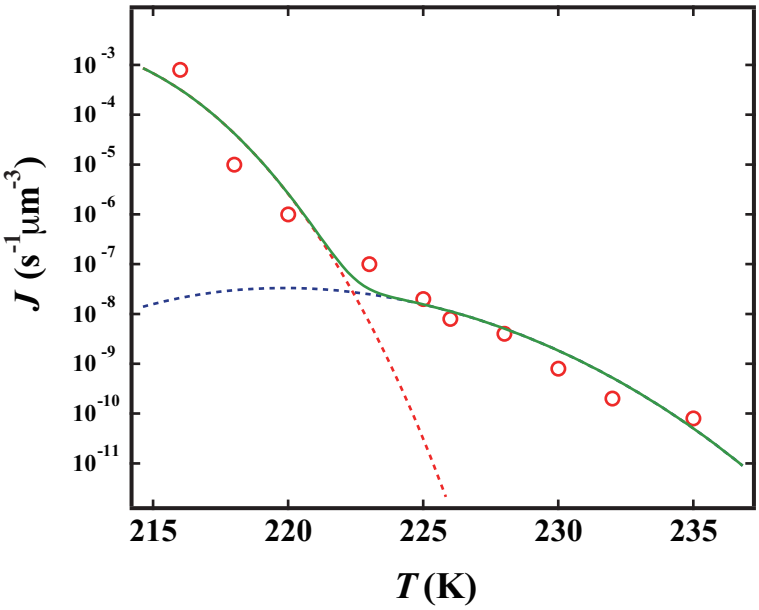

Fig. S4. Fitting the crystal nucleation rate by considering two crystal polymorphs as equation (S2). We obtained from the fitting that k_{n1} = 0.198, k_{n2} = 1.0 $\times$ 10^7, $A = 3.5 \times 10^7$, $B = 1.1 \times 10^7$, and $T_{m2} = 254.7$ K. However, this scenario can be clearly denied by the single melting behavior of only one type of crystal.

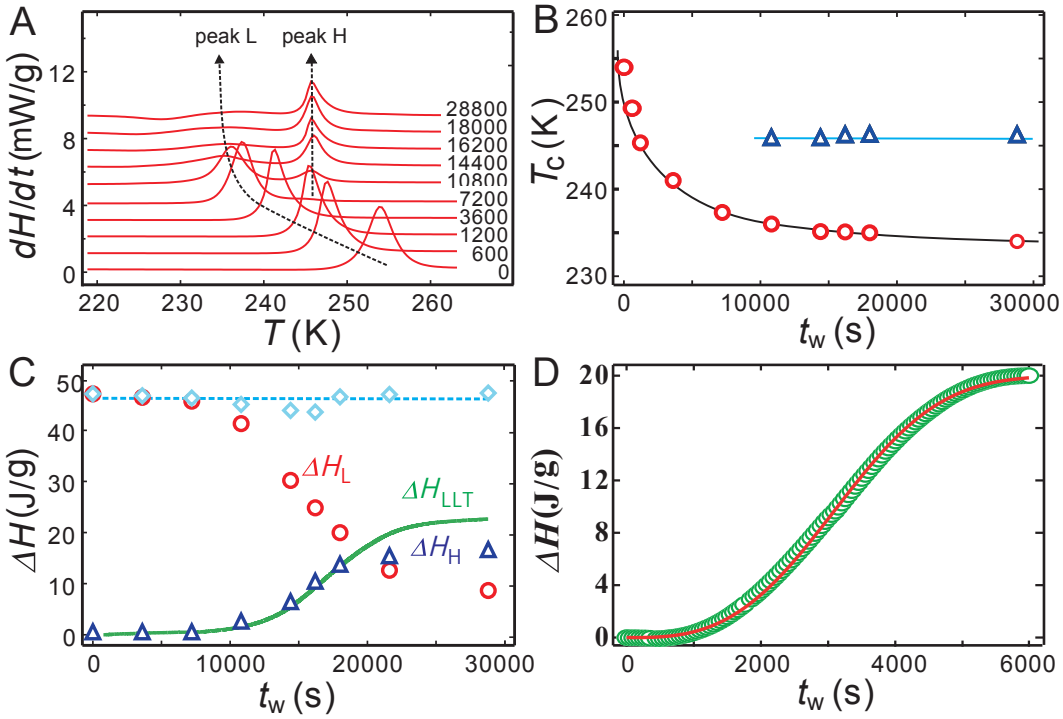

Fig. S5. Separation of crystal nucleation from crystal growth. (A) The heat flux due to crystallization as a function of T during the heating process. We quenched TPP to 213 K, annealed it for $t_{\rm w}$, and then heated it with a rate of 20 K/min. Crystallization takes place during the heating process. The numbers in the figure is $t_{\rm w}$ in the unit of second. For $t_{\rm w} \leq$ 7200 s, only one peak (peak L) appears and its peak temperature decreases with an increase in $t_{\rm w}$. Another peak (peak H) appears around 245 K for $t_{\rm w} \geq$ 10800 s. (B) The $t_{\rm w}$-dependence of the peak temperatures of peak L (circles) and H (squares). (C) The $t_{\rm w}$-dependence of the enthalpy changes associated with peak L (ΔH_L, red circles), peak H (ΔH_H, blue triangles), and LLT (ΔH_{LLT}, green solid curve). The diamond symbols represent the summation of ΔH_L, ΔH_H, and ΔH_{LLT}. (D) The heat evolution during annealing at 243 K after heating from 213 K to 243 K. The solid curve is the fitted Avrami-Kolmogorov equation with the Avrami exponent n = 3.

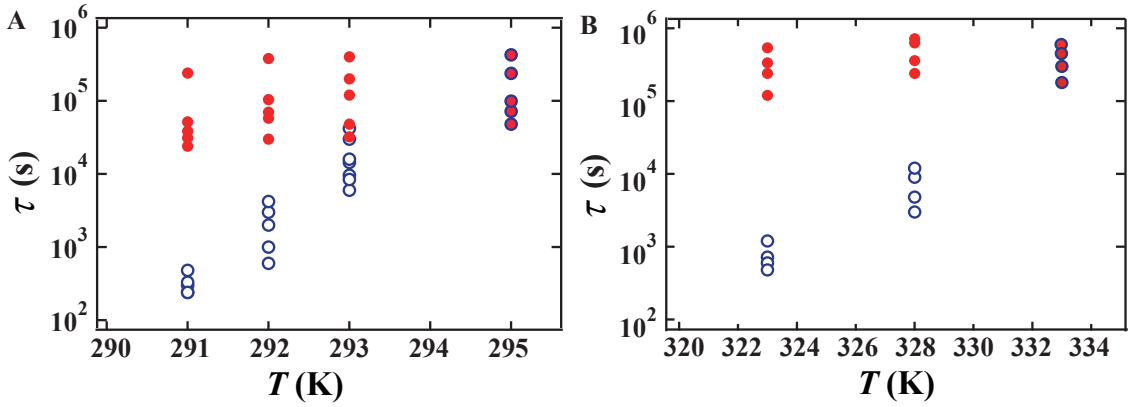

Fig. S6. Incubation times in triphenyl phosphine (TPPN) and polyethylene glycol (PEG). (a) The open circle corresponds to the incubation time when TPPN is annealed and crystallized at $T_{\rm a}$ = 295 K. On the other hand, the filled symbols correspond to the incubation time at a fixed temperature $T_{\rm x}$ =295 K after the liquid is annealed at $T_{\rm a}$ for 5 min. (b) The open circles correspond to the incubation time when the sample is annealed at $T_{\rm a}$, while the filled circle symbols correspond to the incubation time at a fixed temperature $T_{\rm x}$ = 333 K after the sample is annealed at $T_{\rm a}$ for 3 min. We confirmed that these results do not depend on the length of the annealing time.